Annals of Nuclear Energy 73 (2014) 465–477

Contents lists available at ScienceDirect

Annals of Nuclear Energy

journal homepage: www.elsevier.com/locate/anucene

Hydrodynamics of slug flow in a vertical narrow rectangular channel under laminar flow condition

Yang Wang [a], Changqi Yan [a], Xiaxin Cao [a,*], Licheng Sun [b], Chaoxing Yan [a], Qiwei Tian [a]

[a] Fundamental Science on Nuclear Safety and Simulation Technology Laboratory, Harbin Engineering University, Harbin, Heilongjiang 150001, China
[b] State Key Laboratory of Hydraulics and Mountain River Engineering, College of Water Resource & Hydropower, Sichuan University, Chengdu 610065, China

ARTICLE INFO

Article history:
Received 3 February 2014
Received in revised form 12 July 2014
Accepted 15 July 2014
Available online 8 August 2014

Keywords:
Narrow rectangular channel
Slug flow
Length distributions
Taylor bubble length
Liquid slug length

ABSTRACT

The hydrodynamics of gas–liquid two-phase slug flow in a vertical narrow rectangular channel with the cross section of 2.2 mm × 43 mm is investigated using a high speed video camera system. Simultaneous measurements of velocity and duration of Taylor bubble and liquid slug made it possible to determine the length distributions of the liquid slug and Taylor bubble. Taylor bubble velocity is dependent on the length of the liquid slug ahead, and an empirical correlation is proposed based on the experimental data. The length distributions of Taylor bubbles and liquid slugs are positively skewed (log-normal distribution) at all measuring positions for all flow conditions. A modified model based on that for circular tubes is adapted to predict the length distributions in the present narrow rectangular channel. In general, the experimental data is well predicted by the modified model.

1. Introduction

Slug flow is often encountered in many practical applications such as distillation columns, gas absorption units, nuclear reactors, oil–gas pipelines, and steam boilers. The complicated structure of slug flow can be described as a series of slug units, each of which consists of a Taylor bubble with a liquid film around it and a portion of liquid slug behind the Taylor bubble. The evolution of slug flow along a pipeline strongly depends on the relative velocities between the continuous Taylor bubbles. With short separations, trailing Taylor bubbles accelerate and eventually merge with the leading ones (Moissis and Griffith, 1962; Pinto et al., 1998; Aladjem Talvy et al., 2000; Araújo et al., 2013). During the merging process, both the liquid slug and the Taylor bubble increase in length. It is assumed that this process terminates once the liquid velocity profiles at the back of the liquid slug become fully developed and all Taylor bubbles move at the same velocity (Shemer, 2003).

The two-phase slug flow in a narrow rectangular channel is encountered in many important applications, such as high performance micro-electronics, supercomputers, high heat-flux compact heat exchangers and research nuclear reactors with plate type fuels (Satitchaicharoen and Wongwises, 2004). It has been the subject of increased research interest in the past few decades (Griffith, 1963; Maneri and Zuber, 1974; Sadatomi et al., 1982; Mishima et al., 1993; Clanet et al., 2004; Ide et al., 2007; Sowinski et al., 2009; Bhusan et al., 2009; Wang et al., 2013a,b, 2014a,b). However, the majority of the studies are confined to slug flow in circular tubes, a few works deal with the slug flow in narrow rectangular channels.

Several experimental and theoretical works have been reported on the velocity of Taylor bubbles in circular tubes (Dumitrescu, 1943; Davies and Taylor, 1950; Bretherton, 1961; Nicklin et al., 1962; Moissis and Griffith, 1962; White and Beardmore, 1962; Wallis, 1969; Bendiksen and Zuber, 1984; Shemer and Barnea, 1987; Pinto et al., 1998; van Hout et al., 2002; Viana et al., 2003; Zheng and Che, 2006). Nicklin et al. (1962) proposed Eq. (1) to predict the velocity of a single Taylor bubble (V_T) in a moving liquid. It is generally assumed that V_T is a superposition of the drift velocity of a single Taylor bubble in a stagnant liquid (V_0), and a contribution due to the mean liquid velocity (V_m). Eq. (1) has later been applied for predicting the Taylor bubble velocity in continuous slug flow by most researchers, whereas substituting the mean liquid velocity (V_m) by the mixture velocity (j_{TP}), the sum of the liquid and gas superficial velocities (j_L)and (j_G). Then, Eq. (2) results.

$$V_T = C_0 V_m + V_0 \tag{1}$$

$$V_T = C_0 J_{TP} + V_0 \tag{2}$$

* Corresponding author. Tel./fax: +86 0451 82569655.
E-mail addresses: wangyangheu@126.com (Y. Wang), caoxiaxin@hrbeu.edu.cn (X. Cao).

http://dx.doi.org/10.1016/j.anucene.2014.07.022
0306-4549/

Nomenclature

$B_i(t)$	Instantaneous position of the bottom of the i-th liquid slug (m)
C_0	Distribution parameter
Eo	Eotvos number
D	Diameter (m)
D_e	Equi-periphery diameter (m)
D_h	Hydraulic diameter (m)
$F_i(t)$	Instantaneous position of the front of the i-th liquid slug (m)
F_{scale}	Scale factor
G_{TP}	Two-phase mixture mass velocity (kg/(m^2·s))
g	Gravitational acceleration (m/s^2)
h_1, h_2	Distances relative to images bottom edge (pixel)
j_G	Gas superficial velocity (m/s)
j_G^*	Dimensionless gas superficial velocity
j_L	Liquid superficial velocity (m/s)
j_L^*	Dimensionless liquid superficial velocity
j_{TP}	Two-phase superficial velocity (m/s)
L_S	Liquid slug length (m)
$L_{Si}(t)$	Instantaneous length of i-th liquid slug (m)
L_T	Taylor bubble length (m)
$L_{Ti}(t)$	Instantaneous length of i-th Taylor bubble (m)
N_1	Frame of Taylor bubble nose arriving at h_1
N_2	Frame of Taylor bubble nose arriving at h_2
N_3	Frame of Taylor bubble bottom arriving at h_1
N_4	Frame of trailing Taylor bubble nose arriving at h_1
Re_{TP}	Reynolds numbers based on two-phase superficial velocity
Re_{V_s}	Reynolds numbers based on liquid slug velocity relative to Taylor bubble
s	Gap of rectangular channel (m)
V_0	Drift velocity (m/s)
$V_{Fi}(t)$	Instantaneous velocity of the front of the i-th liquid slug (m/s)
V_{max}	Maximum local velocity (m/s)
V_m	Mean liquid velocity (m/s)
V_T	Taylor bubble velocity (m/s)
$V_{Ti}(t)$	Instantaneous velocity of the front of the i-th Taylor Bubble (m/s)
$V_{T\infty}$	Taylor bubble velocity in undisturbed region (m/s)
w	Width of rectangular channel (m)
x	Axial distance from the inlet (m)

Greek letters

α	Average void fraction
α_T	Average void fraction of Taylor bubble region
δ_{fd}	Thickness of narrow side liquid film at the bottom of Taylor bubble (mm)
δ_m	Average liquid film thickness of the narrow side of Taylor bubble region (mm)
μ_L	Liquid phase viscosity (Pa·s)
μ_{TP}	Two-phase viscosity proposed by McAdams et al. (1942) (Pa·s)
ζ	Parameter defined in Eq. (26)
σ	Surface tension (N/s)
π	Circumference ratio
ρ_L	Liquid density (kg/m^3)
ρ_G	Gas density (kg/m^3)
$\Delta\rho$	Density difference between liquid and gas phases (kg/m^3)
τ	Time interval between two frames
ω	Parameter defined in Eq. (26)

Subscripts

G	Gas phase
L	Liquid phase
TP	Two-phase

The value of C_0 is based upon the assumption that the velocity of the Taylor bubble follows the maximum local velocity (V_{max}) in the front of its nose tip, and thus, $C_0 = V_{max}/V_m$ (Nicklin et al., 1962; Bendiksen and Zuber, 1984; Shemer and Barnea, 1987). The value of C_0 therefore equals approximately 1.2 for fully developed turbulent flow and 2.0 for fully developed laminar flow. For the inertia-controlled region when viscosity and surface tension can be neglected (Eotvos number $Eo = g(\rho_L - \rho_G)D^2/\sigma > 70$ and $\rho_L^2 g D^3/\mu_L^2 > 3\times10^5$), White and Beardmore (1962) recommended that the drift velocity V_0 for the vertical tube can be expressed by following equation proposed by Dumitrescu (1943).

$$V_0 = 0.35\sqrt{\Delta\rho g D/\rho_L} \tag{3}$$

where the tube diameter D is taken as the characteristic length, g is the gravitational acceleration, μ_L is the liquid phase viscosity, σ is the surface tension, $\Delta\rho$ is the density difference between the two phases, ρ_G and ρ_L are the gas and liquid density, respectively.

Velocities and characteristic lengths of the Taylor bubble and liquid slug, void fractions in both regions of the slug bubble and liquid slug as well as the drift velocity are required for most classical models of the slug flow in circular tubes (Fabre and Line, 1997). The knowledge of the mean values of the characteristic lengths of Taylor bubble and liquid slug is, however, insufficient for truthful modeling, and the statistical parameters are also required. For circular tubes, experimental investigations on the length distributions of liquid slugs and Taylor bubbles have been carried out for horizontal, inclined and vertical flows (Bernicot and Drouffe, 1989; Barnea and Taitel, 1993; Cook and Behnia, 2000; van Hout et al., 2001, 2003; Shemer, 2003; Zheng and Che, 2006; Mayor et al., 2007a, 2008a,b; Wang et al., 2006; Wang et al., 2009; Xia et al., 2009). The liquid slug length distribution can be described by positively skewed distributions, such as the log-normal, the gamma, or the inverse Gaussian (Dhulesia et al., 1991; Nydal et al., 1992; van Hout et al., 2001, 2003; Shemer, 2003).

Modeling of the evolution of slug flow was undertaken by Bernicot and Drouffe (1989) for the horizontal case and by Barnea and Taitel (1993) for all inclination angles. The latter model was verified against experimental data by Cook and Behnia (2000) and Wang et al. (2006) for the horizontal and slightly inclined cases, by van Hout et al. (2003) for inclined cases, and by Mayor et al. (2007b), Xia et al. (2009) and van Hout et al. (2001) for the vertical cases. All the above models are for the gas–liquid slug flow in the turbulent regime. Predictions by these models compared reasonably well with the experimental data. The dependence of the Taylor bubble velocity on the liquid slug length ahead of it, $V_T = f(L_S)$, should be provided as an input relation to the Barnea and Taitel model. Several researchers proposed the relationship of $V_T = f(L_S)$ based on fitting experimental data. Moissis and Griffith (1962) expressed the function as follows:

$$\frac{V_T}{V_{T\infty}} = 1 + 8\exp\left(-1.06\frac{L_S}{D}\right) \tag{4}$$

where $V_{T\infty}$ is the velocity of the Taylor bubble in the undisturbed condition in which the trailing Taylor bubble is undisturbed by the leading one.

van Hout et al. (2001) modified the correlation of Moissis and Griffith (1962), and it becomes:

$$\frac{V_T}{V_{T\infty}} = 1 + 8\exp\left(-1.5\frac{L_S}{D}\right) + \frac{1}{L_S/D} \tag{5}$$

Mayor et al. (2008b) proposed a new correlation for laminar regime in the main liquid and turbulent regime in the near wake region as follows.

$$\frac{V_T}{V_{T\infty}} = 1 + 0.916\exp\left(-\frac{(L_S/D - 0.811)}{0.775}\right) + 0.02\exp\left(-\frac{(L_S/D - 0.811)}{14.574}\right) \tag{6}$$

For slug flow in a vertical narrow rectangular channel, researchers also have attempted to correlate the Taylor bubble velocity with the same relationship of Eq. (2) (Sadatomi et al., 1982; Ide et al., 2007; Sowinski et al., 2009; Wang et al., 2013a,b, 2014a). Ishii (1977) proposed the following empirical formula of C_0 for rectangular channels.

$$C_0 = 1.35 - 0.35(\rho_G/\rho_L)^{0.5} \tag{7}$$

Since there is not an extensively accepted characteristic length for a rectangular channel, several characteristic lengths and correlations for the drift velocity were put forward (Griffith, 1963; Ishii, 1977; Sadatomi et al., 1982; Clanet et al., 2004). Sadatomi et al. (1982) recommended the equi-periphery diameter (D_e) of a non-circular channel as the characteristic length,

$$D_e = 2(s + w)/\pi \tag{8}$$

where w is the channel width, and s is the gap width, π is the circumference ratio.

And thus Eq. (3) becomes

$$V_0 = 0.35\sqrt{\Delta\rho g D_e/\rho_L} \tag{9}$$

Wang et al. (2014a) investigated the slug flow in a vertical narrow rectangular channel (3.25 mm × 43 mm). They recommend that the Taylor bubble velocity could be well predicted by the Nicklin et al. (1962) correlation provided that C_0 was given by Eq. (7), and V_0 was predicted by Eq. (9).

Up to now, modeling of slug flow in vertical narrow rectangular channels has not been well resolved. The lack of detailed understanding of hydrodynamics of slug flow prevents sufficiently accurate modeling. A deep insight into the characteristics of the slug flow in narrow rectangular channels is needed for understanding the mechanism of slug flow. In particular, the relation of the Taylor bubble velocity with the length of the liquid slug ahead, and the necessity to develop a reliable model for predicting the length distributions of liquid slugs and Taylor bubbles. Thus in this paper, with the help of a high speed video-camera system, an investigation is carried out on the characteristics of slug flow in a vertical narrow rectangular channel with the cross section of 2.2 mm × 43 mm, including the length distributions of liquid slugs and Taylor bubbles along the channel, the relation of the Taylor bubble velocity with the liquid slug length ahead of it.

2. Experiments and data processing

2.1. Experimental apparatus

Fig. 1 shows the schematic diagram of the experimental apparatus. It is mainly composed of a water tank, an air reservoir, a centrifugal pump, an air–water mixing chamber, a test section, a separator, an air compressor and flowmeters. The test section, made of transparent acrylic and mounted vertically on the test platform, is a rectangular duct with a length of 2000 mm and the cross section of 2.2 mm × 43 mm.

Air is supplied by the compressor and stored in the air reservoir. The pressure at gas flowmeter inlet is maintained at gauge pressure of 0.3 MPa by a pressure regulator. Air and water are introduced into the mixing chamber from the centrifugal pump and the air reservoir respectively, to generate uniform mixture. After the mixture flows upwards through the test section, the air is released into atmosphere, while the water returns to the water tank.

The water flow rate is measured in the upstream of the test section by a coriolis mass flowmeter (Promass 83) with an accuracy of ±0.1%. The gas flow rate is also measured at upstream by a mass flowmeter (AALBORG GFM17) with an accuracy of ±1% and the measurement range of 0–0.6 m^3/h. The local pressure is measured at two vertical positions (x = 500 and 1500 mm) on the test section by two pressure transducers (DRUCK UNIK5000) with the same accuracy of ±0.04%. Here, x is the axial distance from the inlet. The test signals of the flowmeters and the pressure transducers are acquired by data acquisition system (sampling frequency is 256 Hz and the uncertainty is ±0.1%) except the water and air temperatures which are tested by a grade-2 standard thermometer with an error of ±0.1 °C. Images with resolution of 1024 pixels in height and 512 pixels in width are digitally recorded by a high speed video camera (Photron FASTCAM SA5 model 1000K-M3) and an image recording software. A back lighting source is applied to obtain gas–liquid interfaces as clear as possible.

2.2. Experimental conditions

The adiabatic air–water flow experiments are performed at atmosphere and room temperature for three combinations of water and gas flow rates. The superficial velocities and the relevant Reynolds numbers are listed in Table 1. The superficial velocities are designed to have laminar regime in the liquid slug between Taylor bubbles and turbulent regime in the wake region of the Taylor bubble. The flow regime in the main liquid is assessed through the values of two-phase Reynolds numbers (Re_{TP}). $Re_{TP} = G_{TP}D_h/\mu_{TP}$ is based on the two-phase mixture mass velocity (G_{TP}), the two-phase viscosity (μ_{TP}) proposed by McAdams et al. (1942) and the hydraulic diameter (D_h). Based on the theoretical analysis of Wang et al. (2012), laminar flow regime is assumed when Re_{TP} is less than 2483. Campos and Guedes de Carvalho (1988) and Pinto et al. (1998) identified three flow patterns (laminar, transition and turbulent) in the wake of Taylor bubble, and recommended that the flow regime in the wake region is assessed computing the Reynolds numbers of the liquid slug $(Re_{V_S}) \cdot Re_{V_S} = (V_{T\infty} - j_{TP})\rho_L D_h/\mu_L$ is based on the liquid slug velocity relative to the Taylor bubble ($V_S = V_{T\infty} - j_{TP}$, where $V_{T\infty}$ is the experimental velocity of Taylor bubble in undisturbed condition), the liquid viscosity (μ_L) and the hydraulic diameter (D_h). According to Pinto et al. (1998), turbulent regime in the wake is acknowledged for $Re_{V_S} > 525$. This criterion for regime transition is extrapolated to the present channel, and it is an approximation. Therefore, as shown in Table 1, the flow regime in the wake of Taylor bubble is always turbulent, and the flow regime in the main liquid is laminar. In addition, for condition (a), the camera frame rate is 250 fps (frames per second). For conditions (b) and(c), the frame rate is 500 fps. The exposure time of images is 1/3000 s for all flow conditions. For each flow condition, 1000 different Taylor bubbles are taken into account. The evolution of the slug flow along the channel is measured by placing the high speed video camera at three different positions (x) along the channel, where x is the axial distance from the inlet. The locations of the measuring positions are listed in Table 2, and they are also shown in Fig. 1.

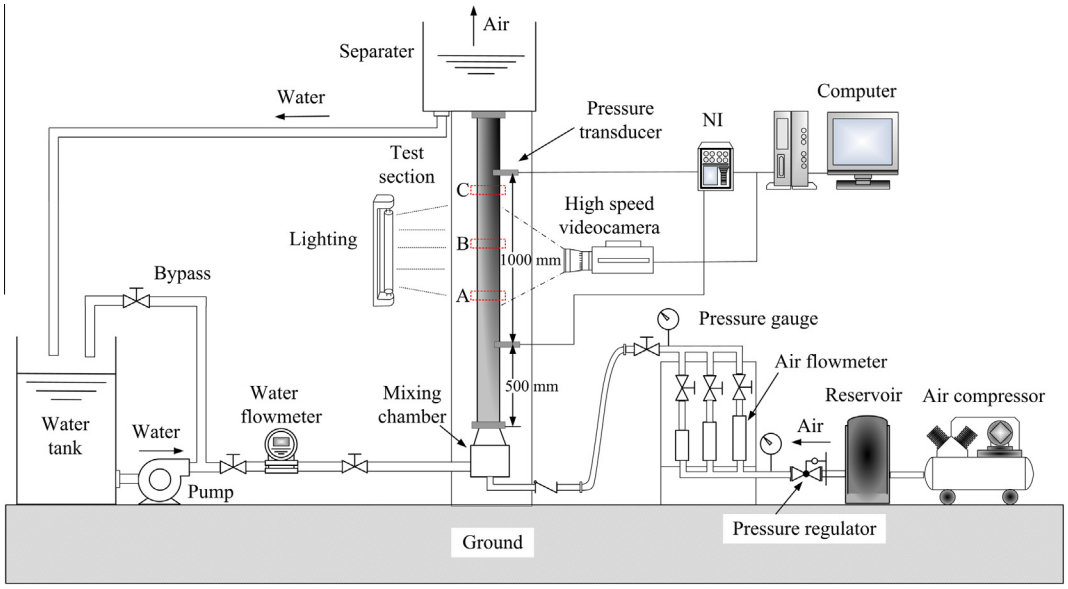

Fig. 1. Schematic diagram of the flow loop.

Table 1
Liquid and gas superficial velocities used in experiments and corresponding Reynolds numbers.

	j_L (m/s)	j_G (m/s)	Re_{TP}	Re_{V_s}
a	0.20	0.18	946	2295
b	0.40	0.18	2118	2487
c	0.40	0.19	2220	2899

Table 2
Sampling positions along the channel.

Position	x (m)	x/D_h	x/D_e	x/w
A	0.830	198	28.8	19.3
B	1.075	257	37.4	25.0
C	1.320	316	45.9	30.7

2.3. Data processing

The recorded images are processed by a human operator using an image processing software (Photron FASTCAM Viewer). The data processing is similar to Wang et al. (2014a) and Yan et al. (2014). Firstly, a scale factor is given for converting the image unit into the actual value, which is defined as follows:

$$F_{scale} = \frac{\text{practical width of the test section}}{\text{width of the test section in the image}} \tag{10}$$

Fig. 2 shows four typical frames of N_1, N_2, N_3 and N_4 in time sequence extracted from a small period of high-speed video film. Thus, the velocity of a Taylor bubble (V_T) can be obtained by analysis of a series of succeeding images.

$$V_T = \frac{F_{scale}(h_2 - h_1)}{\tau(N_2 - N_1)} \tag{11}$$

where τ is the time interval between two continuous frames; h_1 and h_2 are the distances relative to images bottom edge; N_1 and N_2 are the frames of Taylor bubble nose arriving at h_1 and h_2, respectively.

The Taylor bubble length (L_T) could then be calculated by multiplying the residence time of the Taylor bubble over h_1 by the Taylor bubble nose velocity.

$$L_T = \tau\, V_T(N_3 - N_1) \tag{12}$$

where N_3 is the frame of Taylor bubble bottom arriving at the elevation h_1.

Similarly, the liquid slug length could be easily calculated. Due to the complex behavior of the Taylor bubble tail, the length of liquid slug (L_S) is calculated according to the nose velocity of the leading Taylor bubble.

$$L_S = \tau\, V_T(N_4 - N_3) \tag{13}$$

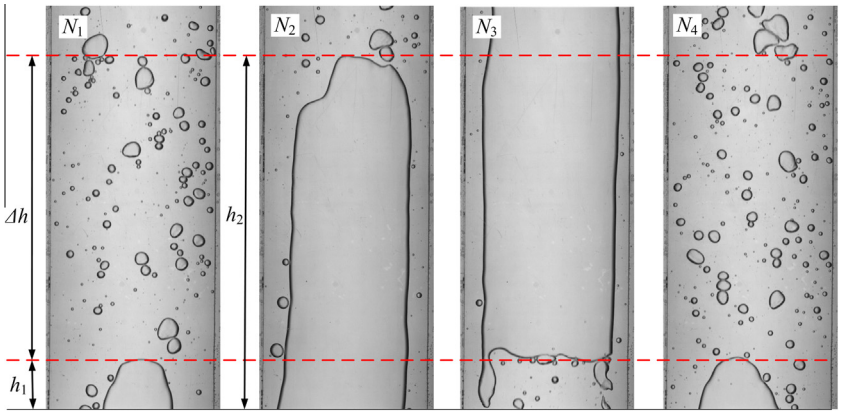

Fig. 2. Typical images of data processing.

where N_4 is the frame of a trailing Taylor bubble nose arriving at h_1.

3. Modeling for the length distributions of the liquid slug and Taylor bubble

In this section, a model for predicting liquid slug length in the narrow rectangular channel is adapted based on those for circular tubes (Bernicot and Drouffe, 1989; Barnea and Taitel, 1993; Cook and Behnia, 2000). The model tracks the front and bottom of liquid slugs along the channel and allows liquid slugs to collapse or grow depending on their length and that of the preceding liquid slug. The length distributions of the Taylor bubble and liquid slug at any axial location along the channel can be ascertained. In addition, the bubble expansion and the oscillation of the pressure and flow rates are neglected in the present model.

Fig. 3 shows a schematic structure of the liquid slugs as they are generated at the entrance. The model calculates the instantaneous position of the front ($F_i(t)$) and bottom ($B_i(t)$) of the i-th liquid slug as it moves downstream, and the instantaneous velocities of front and bottom of liquid slug are $V_{Fi}(t)$ and $V_{Ti}(t)$, respectively. The last liquid slug, the liquid slug which is either in the process of entering the channel or has just entered the channel, is designated as number n. The front of the first slug ($F_1(t)$) is assumed to be traveling behind a liquid slug of stable length, so that the front of this first liquid slug moves at a stable velocity $V_{T\infty}$. $V_{T\infty}$ could be reliably predicted by the Nicklin et al. (1962) correlation provided that C_0 is given by Eq. (7) and V_0 is predicted by Eq. (9) (see the discussion in section 4.1.3).

The bottom of each liquid slug moves with a velocity dependent on its length, and the relationship of $V_T = f(L_S)$ (Eq. (25) in the section 4.1.2) is used to determine this liquid slug bottom instantaneous velocity $V_{Ti}(t)$. The instantaneous lengths of the i-th liquid slug ($L_{Si}(t)$) and Taylor bubble ($L_{Ti}(t)$) could be calculated by Eqs. (14) and (15), respectively. According to the analysis of the bubble-to-bubble interaction curve, a given trailing Taylor bubble flows less than 0.02% faster than the leading one, provided that the liquid slug between them is longer than 10 w (see the discussion in section 4.1.2). Therefore for a liquid slug longer than 10 w, $V_{Ti}(t)$ is set equal to the velocity of the first liquid slug $V_{T\infty}$. The model ignores any gas expansion within the Taylor bubbles. Therefore the instantaneous velocity of the front of each liquid slug is thus equal to that of the preceding liquid slug bottom (as Eq. (16)).

$$L_{Si}(t) = F_i(t) - B_i(t) \tag{14}$$

$$L_{Ti}(t) = B_i(t) - F_{i+1}(t) \tag{15}$$

$$V_{Fi}(t) = V_{Ti-1}(t) \tag{16}$$

The change of the positions of each liquid slug with a small increment in time (Δt) is calculated by the model as follow, and Δt in the program of present model sets as 0.001 s.

$$F_i(t+\Delta t) = F_i(t) + V_{Fi}\Delta t \tag{17}$$

$$B_i(t+\Delta t) = B_i(t) + V_{Bi}\Delta t \tag{18}$$

The increase or the decrease in the liquid slug length as it moves depends on the relative velocity between its front and its back ($V_{Fi}(t) - V_{Ti}(t)$). When this value is positive the slug length increases, and vice versa. Since $V_{Fi}(t) = V_{Ti-1}(t)$, and $V_{Ti}(t)$ depends on the liquid slug length, short liquid slugs behind longer ones tend to decrease in length while long liquid slugs behind shorter ones grow in length. As a result, short liquid slugs with lengths decreasing eventually disappear and are swallowed by the liquid slug behind them, while the two succeeding Taylor bubbles coalesce (Barnea and Taitel, 1993).

In the model, it is assumed that a set of short liquid slugs with random lengths are generated at the channel entrance. The length of the Taylor bubble behind each generated liquid slug is assumed to be associated with the liquid slug length by the following relation.

$$\alpha = \frac{j_G}{V_T} = \frac{\alpha_T L_T}{L_T + L_S} \tag{19}$$

where α is the average void fraction, α_T is the average void fraction of the Taylor bubble region.

In the model of Barnea and Taitel (1993), the thickness of the film around the Taylor bubble is neglected, and Eq. (19) then becomes

$$\alpha = \frac{j_G}{V_T} \approx \frac{L_T}{L_T + L_S} \tag{20}$$

In the present model, the film thickness of the Taylor bubble region is not neglected. Based upon the observations of Mishima et al. (1993) and the measurement of the film thickness with conductivity probes by Wilmarth and Ishii (1997), it is assumed that the liquid film on the wide side walls can be neglected compared with that of the narrow side for slug flow. This assumption is valid for the rectangular channel with the gap smaller than about 2.4 mm (Hibiki and Mishima, 2001). Since the gap of the present channel is 2.2 mm, the assumption is also valid. Therefore, the average void fraction (α_T) of the Taylor bubble region could be calculated by

$$\alpha_T = 1 - 2\frac{\delta_m}{w} \tag{21}$$

where δ_m is the average liquid film thickness of the narrow side of the overall Taylor bubble region. Since the liquid film of narrow side rapidly decreases along the Taylor bubble and approximates a constant value, δ_m is almost equal to the thickness of the liquid film at the bottom of the Taylor bubble (δ_{fd}) (Wang et al., 2014a). Wang et al. (2014a) recommend that δ_{fd} could be predicted by

$$\delta_{fd}/w = 0.1183\, j_G^{*-0.267} j_L^{*0.315} \tag{22}$$

where j_G^* and j_L^* are dimensionless gas and liquid superficial velocities, given by

$$j_L^* = j_L/\sqrt{gD_h} \tag{23}$$

$$j_G^* = j_G/\sqrt{gD_h} \tag{24}$$

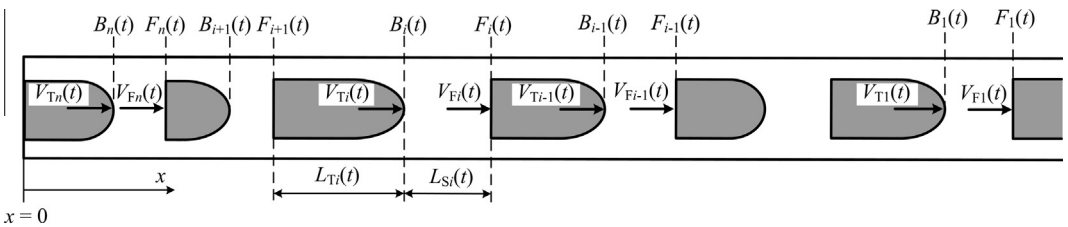

Fig. 3. Schematic of slug distribution at the entrance.

In the program of present model, when a liquid slug have traveled away from the entrance with a distance equal to the Taylor bubble length, the next liquid slug front is then introduced into the channel. When $B_i(t)$ approaches $F_i(t)$, the liquid slug collapse, and the number of each liquid slug behind it is decreased by one. The model is encoded, the lengths of each liquid slug and Taylor bubble passing a set position are recorded and their length distributions at various axial locations could be compared.

4. Experimental data

4.1. Taylor bubble velocity

4.1.1. Taylor bubble velocity along the channel

Fig. 4 shows the velocities of Taylor bubbles as a function of position along the channel for various flow conditions. The Taylor bubble velocities are the average values of all experimental data for each experimental condition (about 1000 Taylor bubbles for one experimental condition). In addition, the gas and liquid superficial velocities are calculated according to the pressure of the position B. The shapes of the curves in Fig. 4 are almost horizontal lines. This indicates that the increase of the Taylor bubble velocity along the channel (between positions A and C in Fig. 1) is insignificant. Since the pressure drop along the channel (between positions A and C) is about several kilopascal, the increasing in the Taylor bubble velocity due to the gas expansion is about 0.02 m/s (below 3% of the Taylor bubble velocity at position A). And according to the error analysis of the data processing, the experimental results of the Taylor bubble velocity are in a 2.9% uncertainty. The Taylor bubble velocity increasing due to the gas expansion and the measurement uncertainty in the Taylor bubble velocity are in the same magnitude. Therefore, the effect of gas expansion on the Taylor bubble velocity (between positions A and C) is unnoticed in the experimental results.

4.1.2. The relationship of the Taylor bubble velocity with the liquid slug length ahead of it

Fig. 5 shows the averaged Taylor bubble velocities as a function of the liquid slug lengths ahead of them. For the purpose of generalization, Taylor bubble velocities are normalized by the Taylor bubble velocities in undisturbed conditions ($V_{T\infty}$) ($V_{T\infty}$ is discussed subsequently), and the liquid slug lengths are normalized by the channel width (w). By averaging the normalized velocities, for each slug length class (classes of 0.5 w), for the nine experimental conditions (three flow conditions × three measured positions), the

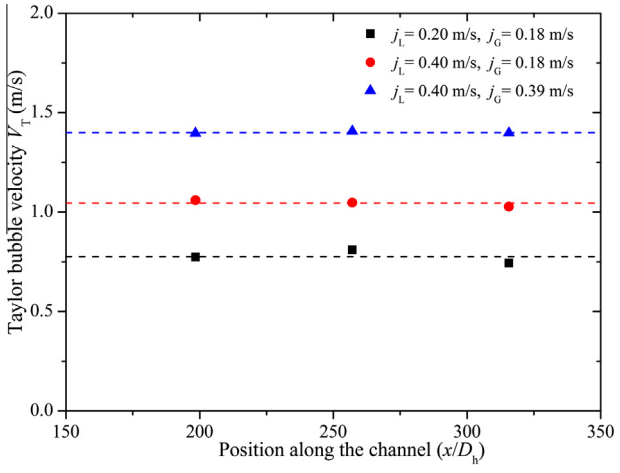

Fig. 4. Variation along the channel of the Taylor bubble velocity.

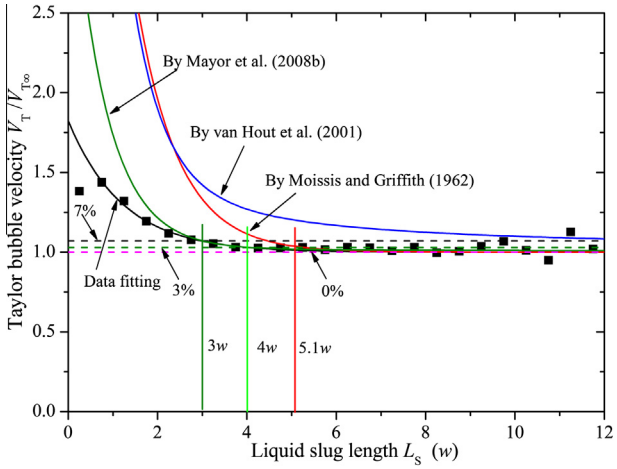

Fig. 5. Variation of averaged Taylor bubble velocities with the liquid slug lengths ahead of them.

averaged Taylor bubble velocity in Fig. 5 is obtained. In addition, the correlations mentioned previously (Moissis and Griffith, 1962; van Hout et al., 2001; Mayor et al., 2008b) and the best fitted curve (Eq. (25)) are also shown in Fig. 5.

$$\frac{V_T}{V_{T\infty}} = 1 + 0.825 \exp\left(-0.824 \frac{L_S}{w}\right) \tag{25}$$

As shown in Fig. 5, there exists a significant acceleration of Taylor bubbles for liquid slug lengths ahead of them shorter than 3 w. The maximum normalized Taylor bubble velocity is about 1.5. The velocities of the Taylor bubbles gradually decrease with increasing liquid slug length ahead of them and approximate the undisturbed Taylor bubble velocity $V_{T\infty}$. The reason is discussed as follow. The velocity of a trailing Taylor bubble is related to the maximum local liquid velocity ahead of it. The velocity field behind a leading Taylor bubble changes from a jet flow pattern in the near-wake region to a fully developed flow in the region far away from the leading Taylor bubble. Thus, the maximum local liquid velocity decreases with the distance from the leading Taylor bubble. Therefore, Taylor bubbles behind short liquid slugs travel much faster than those behind long ones. The Taylor bubbles are accelerated in the wake region, while their velocities reduce exponentially as the separation between the leading and trailing ones increases (Moissis and Griffith, 1962; Shemer and Barnea, 1987). However, for very short liquid slug length (below 0.5 w), the Taylor bubble velocity abruptly decreases. This phenomenon may be explained by the fact that during coalescence process of two succeeding Taylor bubbles, there exists a small liquid 'bridge' between them, and the trailing bubble travels approximately with the same velocity of the leading one, as visualized by the recorded video film. These are consistent with results in circular tubes (van Hout et al., 2001; Mayor et al., 2008b; Araújo et al., 2013).

The analysis of the Eq. (25) indicates that 3–4 w is the threshold of the slug length for two succeeding Taylor bubbles with strong interaction (in this range, the Taylor bubbles rise between 7% and 3% faster than the undisturbed Taylor bubbles). In addition, this interaction is slight for liquid slugs longer than 5.1 w. Indeed, for L_S = 5.1 w and 10 w the trailing Taylor bubbles rise about 1.2% and 0.02% faster than the undisturbed ones. For very long liquid slug lengths, due to insufficient ensemble size at these conditions, considerable scatter in the Taylor bubble velocity data is observed. The measured Taylor bubble velocity is predicted quite well by Mayor et al. (2008b) correlation, whereas for $L_S/w < 3$, it is overpredicted. The correlations of Moissis and Griffith (1962) and van Hout

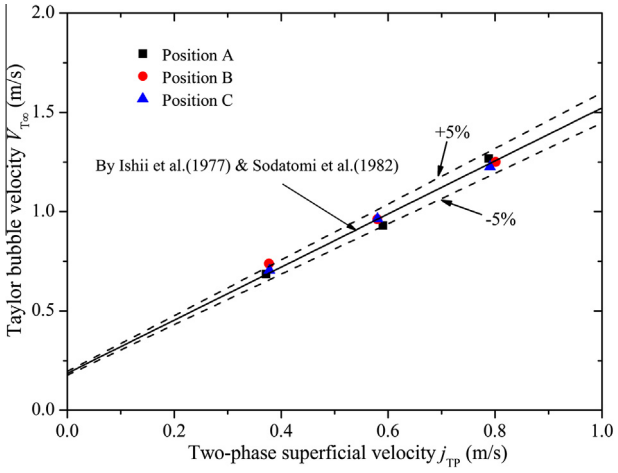

Fig. 6. Variation of undisturbed Taylor bubble velocities with two-phase superficial velocity.

et al. (2001) much overpredict the Taylor bubble velocity. Since above correlations are proposed on the basis of experimental data from circular tubes, they are not suitable for present rectangular channel.

4.1.3. Taylor bubble velocity in undisturbed condition

The velocity of Taylor bubble in undisturbed conditions ($V_{T\infty}$) is a parameter of significant importance for slug flow. For the purpose of assuring undisturbed Taylor bubble velocity, only Taylor bubbles flowing behind liquid slugs longer than 5.1 w are considered. The establishment of 5.1 w as the minimum liquid slug length for the computation of $V_{T\infty}$ results from a balance between representatively and accuracy. Indeed, computing $V_{T\infty}$ based only on Taylor bubbles flowing behind longer liquid slugs would jeopardize the representatively of the estimates, as they would be based on a relatively small sample of Taylor bubbles. Besides, according to the bubble-to-bubble interaction curve (Eq. (25)), a given trailing Taylor bubble flows less than 1.2% faster than the leading one, provided that the liquid slug between them is longer than 5.1 w. Thus, although $V_{T\infty}$ obtained in these conditions are slightly overestimated, the increasing representatively of the estimates clearly makes up for the eventual drawback in accuracy. This method is similar to Mayor et al. (2007a, 2008a,b).

The variation of Taylor bubble velocities ($V_{T\infty}$) in undisturbed regions against the two-phase superficial velocity (j_{TP}) is shown in Fig. 6. $V_{T\infty}$ is the average value of all data for $L_S/w > 5.1$ and obtained for continuous slug flow. A comparison is made with the predicted $V_{T\infty}$ according to the Nicklin et al. (1962) correlation with C_0 given by Ishii (1977), and the drift velocity V_0 predicted by correlations proposed by Sadatomi et al. (1982). It is shown that the correlation predicts the measured data well with the relative deviations below 5% for all flow conditions. Thus, $V_{T\infty}$ could be reliably predicted by the Nicklin et al. (1962) correlation provided that C_0 is given by Eq. (7) and V_0 is predicted by Eq. (9).

4.2. Length distributions of Taylor bubble and liquid slug

Fig. 7 shows the liquid slug length distributions at various positions along the channel for various flow rates. The bin size in the histograms is half channel width 0.5 w, and the histograms show the percentage of total number of liquid slugs. The length distributions of Taylor bubble are shown in Fig. 8. The mean value (L_{Smean} and L_{Tmean}) and the standard deviation (Std. Dev.) of liquid slug and Taylor bubble lengths are also presented in Figs. 7 and 8, respectively. In order to clearly show the evolution of the slug flow, mean values of the liquid slug and Taylor bubble lengths along the channel for various flow rates are shown in Fig. 9.

The coalescence process along the channel results in a gradual increase of the mean values of the Taylor bubble and liquid slug lengths. Accordingly, the distributions become more flat with

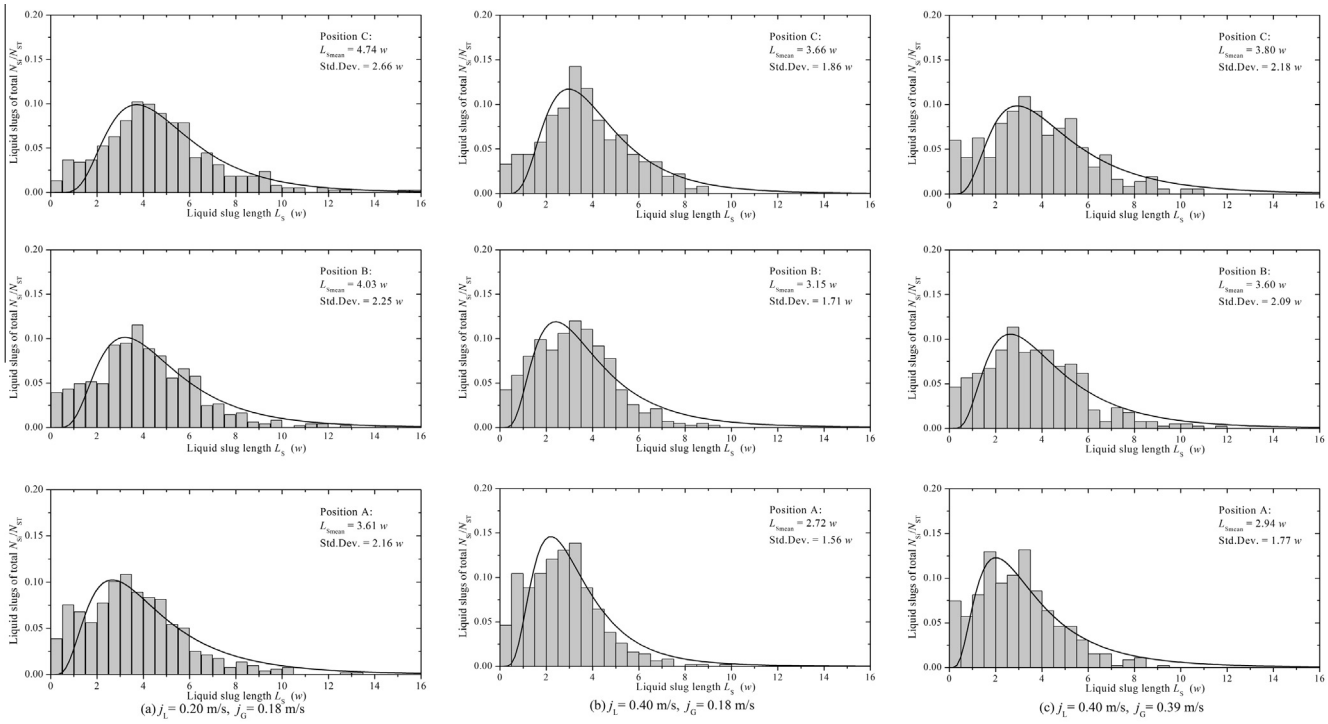

Fig. 7. Liquid slug length distributions at various positions along the channel for various flow rates: (a) first column for j_L = 0.20 m/s, j_G = 0.18 m/s; (b) second column for j_L = 0.40 m/s, j_G = 0.18 m/s; (c) third column for j_L = 0.40 m/s, j_G = 0.39 m/s.

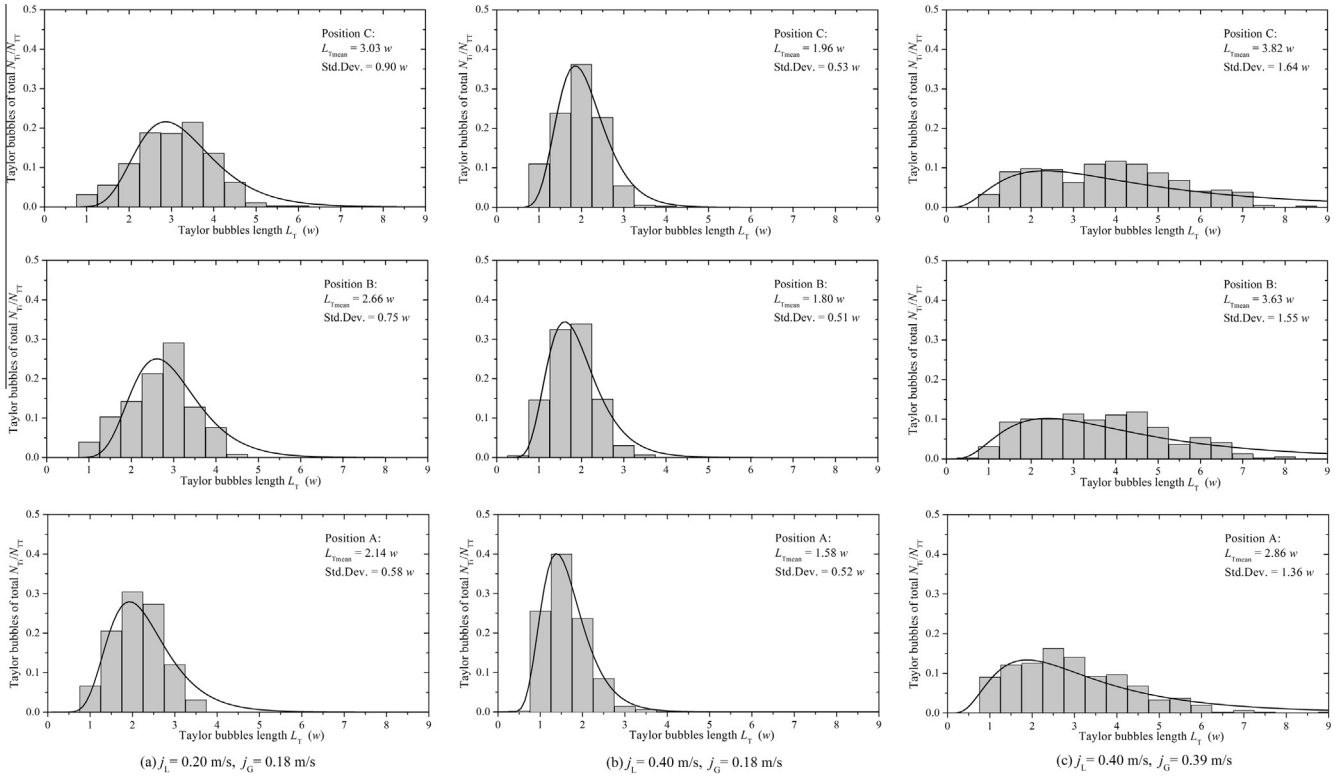

Fig. 8. Taylor bubble length distribution at various positions along the channel for various flow rates: (a) first column for j_L = 0.20 m/s, j_G = 0.18 m/s; (b) second column for j_L = 0.40 m/s, j_G = 0.18 m/s; (c) third column for j_L = 0.40 m/s, j_G = 0.39 m/s.

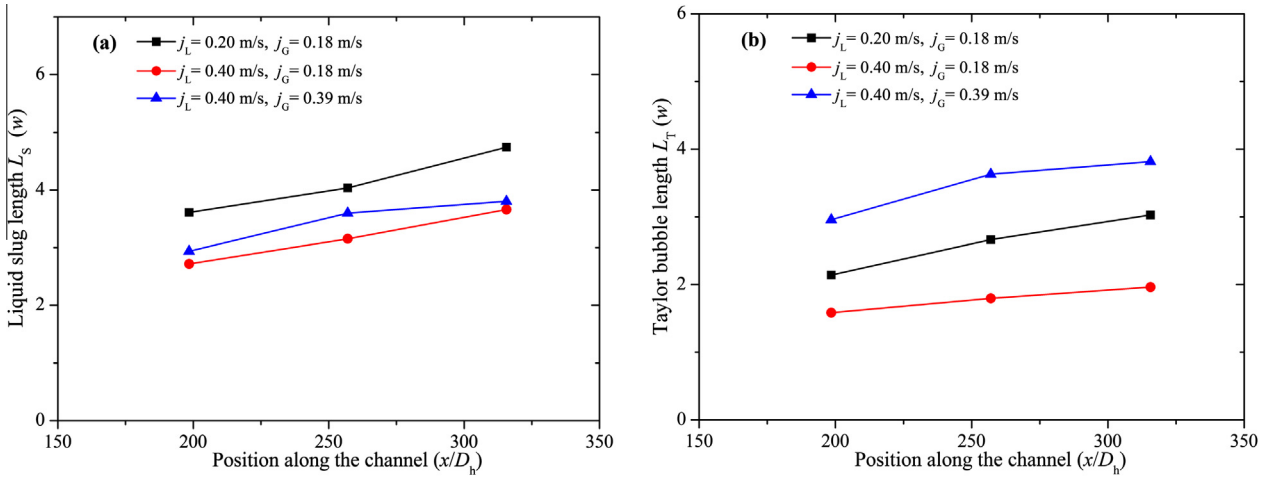

Fig. 9. Average liquid slug and Taylor bubble lengths as a function of the position along the channel for various flow rates: (a) liquid slug length; (b) Taylor bubble length.

increasing distances from the channel inlet. As shown in Figs. 7 and 8, it is clearly seen that the length distributions of liquid slug and Taylor bubble are both visibly right skewed (tails extending to large values). A best fit to the log-normal distribution is performed, and the resulting distribution curve is also plotted in these figures (see the solid line). The probability density function of log-normal distribution (Miller and Freund, 1965) is as follow

$$f(x) = \frac{1}{\sqrt{2\pi}\omega(L_S/0.5w)} \exp -\frac{1}{2}\left[\frac{\ln(L_S/0.5w) - \xi}{\omega}\right]^2 \quad (26)$$

where $x > 0$ and $\omega > 0$. The parameters ω and ζ are listed in Table 3 for all cases.

As show in Fig. 7, at the higher measuring position (position C), there is still a significant percentage of short liquid slugs, which implies that several coalescences occur above this position. Thus, the slug flow in present channel is undeveloped continuous slug flow. It can be seen from Figs. 7 and 9a that at each position the mean liquid slug lengths seem to be almost insensitive to the gas flow rate, but depend on the liquid flow rate. Contrary to this, the mean Taylor bubble lengths depend on the gas and liquid flow rates (see Figs. 8 and 9b). These are similar to the results in the circular tubes (van Hout et al., 2001, 2003; Mayor et al., 2007a, 2008a,b).

For a given gas superficial velocity j_G, the increase in liquid superficial velocity j_L results in the formation of shorter Taylor

Table 3
Parameters ω and ζ of the log-normal fit.

j_L (m/s)	0.20			0.40			0.40		
j_G (m/s)	0.18			0.18			0.39		
Position	A	B	C	A	B	C	A	B	C
Liquid slug length									
ω	0.61	0.53	0.48	0.54	0.59	0.51	0.65	0.6	0.58
ζ	2.04	2.14	2.24	1.77	1.91	2.04	1.82	2.02	2.11
Taylor bubble length									
ω	0.35	0.29	0.31	0.34	0.34	0.31	0.65	0.66	0.72
ζ	1.47	1.74	1.84	1.13	1.28	1.84	1.74	2	2.05

bubbles and longer liquid slugs at the entrance. This means that there is an inlet positive-slope trend for the liquid slug length L_S (when L_S is plotted against j_L). Since less coalescence occurs to Taylor bubbles with longer distances between each other, this inlet trend of L_S results in a decrease in the number of coalescences occurring along a given channel length. Due to a decrease in the number of coalescences, the mean lengths of Taylor bubble and liquid slug decrease. Thus, there is a competition between two effects: the inlet trend effect (which implies a decrease in L_T and an increase in L_S) and the coalescence effect (which implies a decrease in both variables). Figs. 7a and b, 8a and b and 9 indicate that the coalescence effect is dominant in the variation of L_T and L_S with j_L. Therefore the standard deviation and mean values of L_T and L_S decrease with increasing j_L, and flow is more stable. Similar

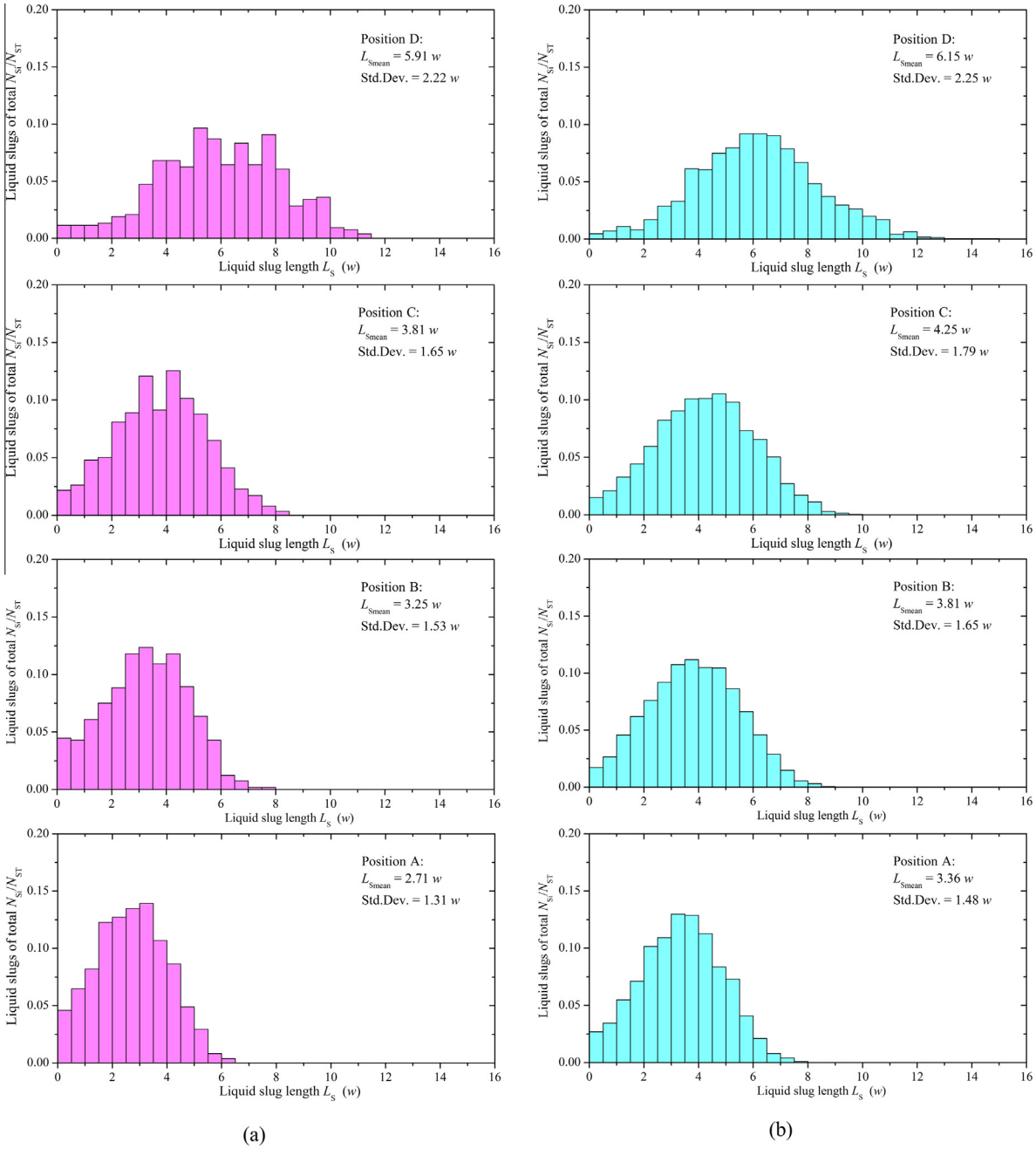

Fig. 10. Computed liquid slug length distributions along the channel for different inlet liquid slug length distributions for j_L = 0.40 m/s, j_G = 0.39 m/s: (a) first column for the uniform random inlet slug lengths between 0.5 and 1 w; (b) second column for the uniform random inlet slug lengths between 1 and 2 w.

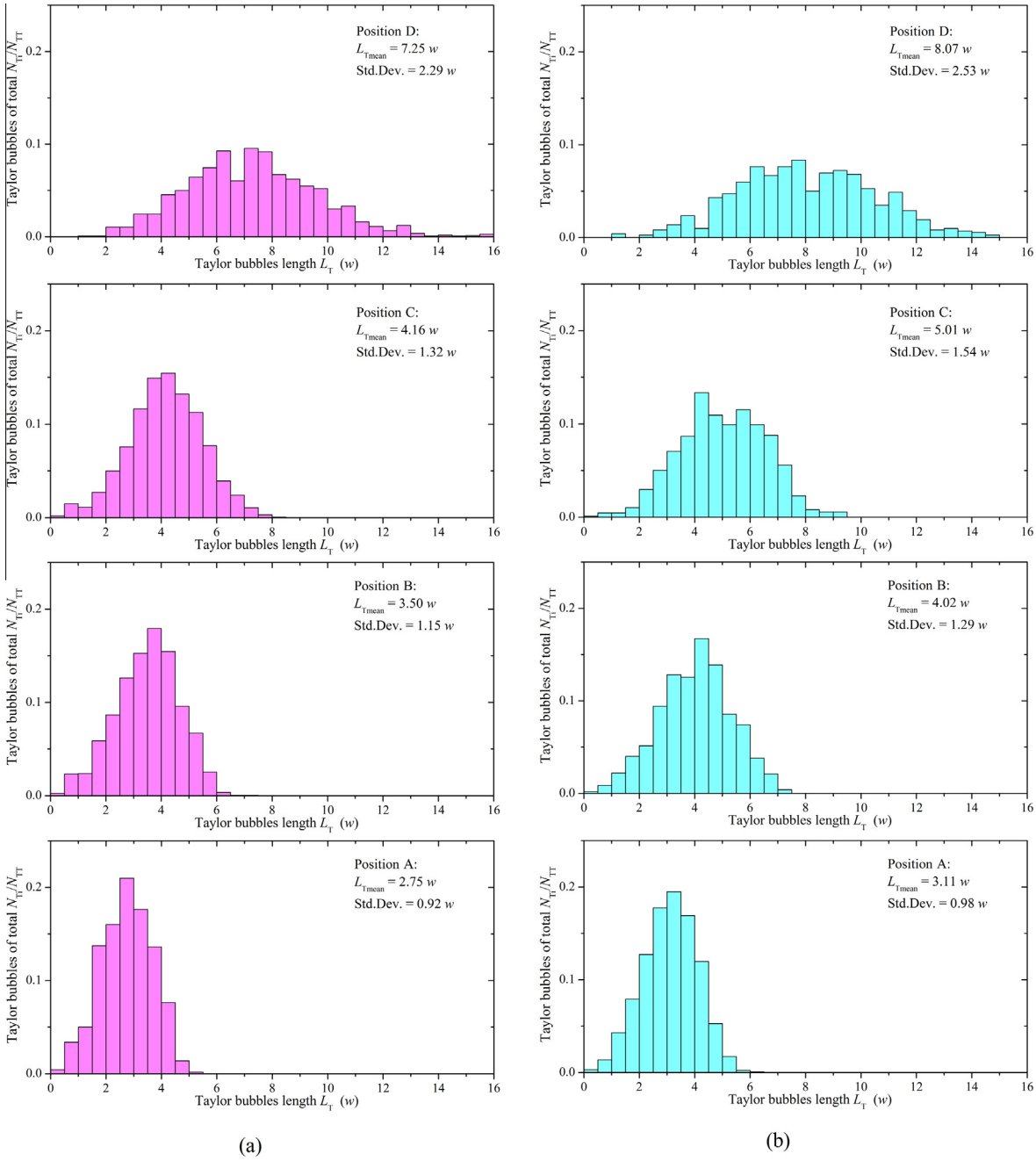

Fig. 11. Computed Taylor bubble length distributions along the channel for different inlet liquid slug length distributions for j_L = 0.40 m/s, j_G = 0.39 m/s: (a) first column for the uniform random inlet slug lengths between 0.5 and 1 *w*; (b) second column for the uniform random inlet slug lengths between 1 and 2 *w*.

observations are reported by Mayor et al. (2007a, 2008a,b) and van Hout et al. (2001, 2003).

For a given liquid superficial velocity j_L, the inlet negative-slope trend effect (when L_S is plotted against j_G) implies that longer Taylor bubbles and shorter liquid slugs results from increasing j_G. Since the Taylor bubbles coalesce more with shorter distances between each other, both of L_T and L_S are expected to increase along a given channel length due to the more frequent coalescence. While both effects (the inlet trend and the coalescence) point towards an increase of L_T with j_G, the influence of the two effects on the variation of L_S is opposite. Thus, the variation of L_S depends on the competition between the two effects. Figs. 7b and c, 8b and c and 9a indicate that the influence of the two opposite effects on L_S is similar. Therefore, the variation of L_S seem to be almost insensitive to j_G, the standard deviation and mean values of L_T increase with increasing j_G, and flow is less stable. Similar observations are reported by Mayor et al. (2007a, 2008a,b) and van Hout et al. (2001, 2003).

5. Slug flow simulation

5.1. Influence of the inlet slug length distribution

Since the channel length is too short to achieve stabilization length distributions of Taylor bubble and liquid slug, the slug flow in present experiment is undeveloped. The simulation results may be dependent on the slug length distributions at the entrance. Therefore, the influence of the initial distributions of liquid slug

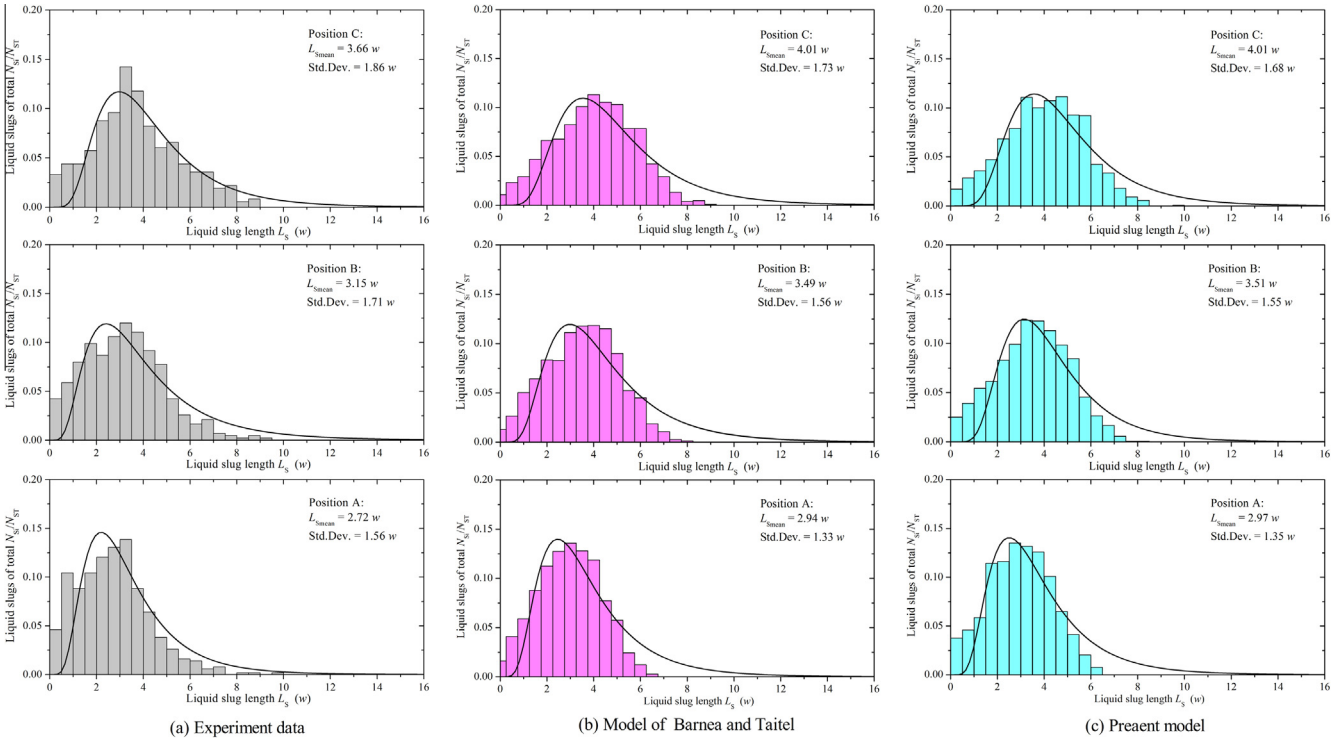

Fig. 12. Comparison between measured and computed liquid slug length distributions for different positions along the channel for j_L = 0.40 m/s, j_G = 0.18 m/s: (a) first column for the experiment data; (b) second column for results of Barnea and Taitel model; (c) third column for results of present model.

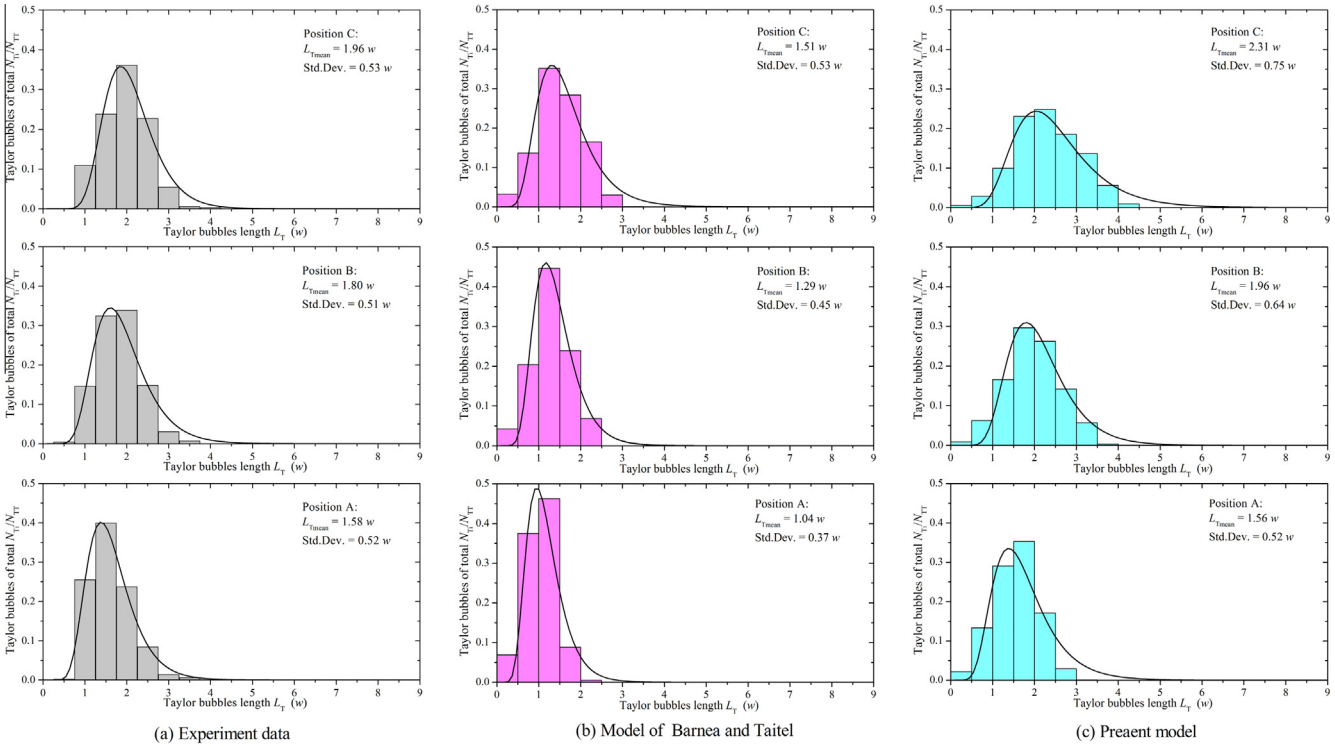

Fig. 13. Comparison between measured and computed Taylor bubble length distributions for different positions along the channel for j_L = 0.40 m/s, j_G = 0.18 m/s: (a) first column for the experiment data; (b) second column for results of Barnea and Taitel model; (c) third column for results of present model.

is investigated. The channel length for simulation sets as 4 m. In order to obtain a meaningful statistical distribution, 10,000 liquid slugs are calculated at the channel entrance. The computed liquid slug length distributions along the channel for two different inlet liquid slug length distributions are shown in Fig. 10. The first column of the figure is for the uniform random inlet slug lengths between 0.5 and 1 *w*, and the second column is for the uniform random inlet slug lengths between 1 and 2 *w*. In addition, the

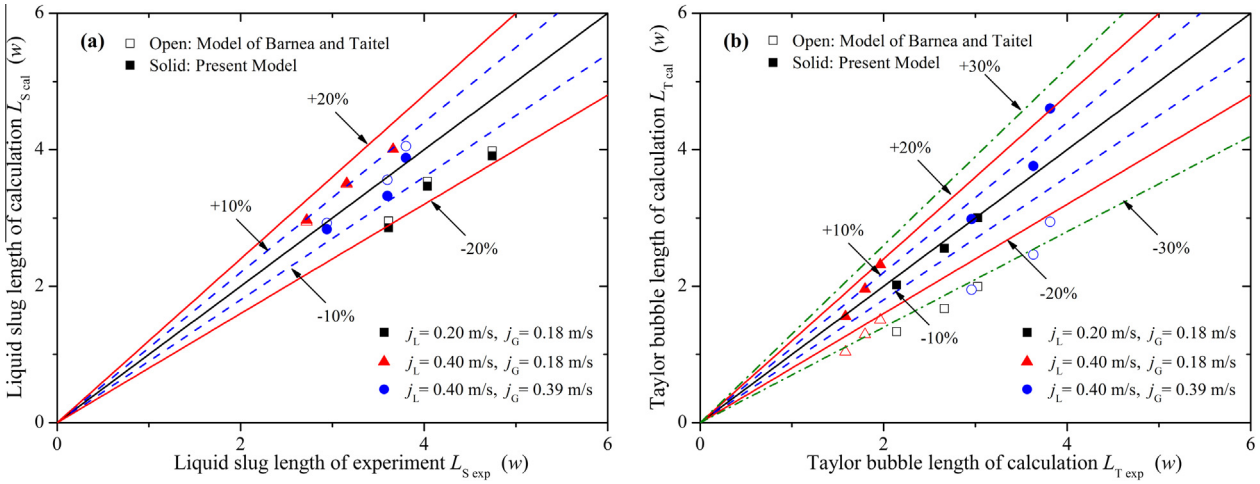

Fig. 14. Comparison between measured and computed average lengths of Taylor bubble and liquid slug: (a) liquid slug length; (b) Taylor bubble length.

length distributions at four positions (A, B, C and D) along the channel are presented in the Fig. 10. The positions of A, B and C are listed in Table 2, and they are in the entrance region. Based on the simulation results of Mayor et al. (2007b), the entrance length of slug flow for simulations is in the range of 50–70 *D* (*D* is the tube diameter). Thus the position D sets as 3000 mm from the entrance (about 70 *w* from inlet), and the entrance effect could be neglected. In corresponding, the simulation results of the Taylor bubble length distributions are shown in Fig. 11. As shown in Figs. 10 and 11, the development and the shape of the length distributions of two different inlet slug lengths are similar. The computed average values of liquid slug length and Taylor bubble length increase with the average inlet slug lengths increasing, the length discrepancy between two different initial liquid slug length distributions reduce along the channel, and the effect of the initial liquid slug distributions could be neglected at the position D (70 *w* from inlet).

5.2. Simulation results versus experimental data

In the simulation, 10,000 liquid slugs are calculated at the channel entrance, and the initial liquid slug lengths are in a uniform distribution between 0.5 and 1 *w* for all the simulation conditions. The predicted and measured results of the length distributions of the liquid slug and Taylor bubble for j_L = 0.40 m/s, j_G = 0.18 m/s for three measurement positions are shown in Figs. 12 and 13, respectively. The first column of Figs. 12 and 13 presents the length distributions of experimental data. The second and third columns show the predicted results of the Barnea and Taitel model and the present model, respectively. As shown in Fig. 12, the length distributions of liquid slug for the models differ a bit of the log-normal distribution, and the percentage of longer liquid slug of the simulation results is lower than that of the experimental data. In general, there is a good agreement between the development and the shape of the predicted and the measured distributions of liquid slug length for both models. Fig. 13 indicates that the present model well predicts the development and the shape of the distributions of Taylor bubble length. However, due to unsuitably using Eq. (20), the distributions predicted by the Barnea and Taitel model tend to become more peaked, and the mean values are underpredicted. In order to clearly show the comparison between the measured and computed mean lengths of liquid slug and Taylor bubble, the simulation results versus the experimental data for three flow conditions and three positions are also shown in Fig. 14. For the present model, the overall mean relative deviations of average lengths of liquid slug and Taylor bubble are 10.37% and 5.58%, respectively. As discussed above, it may be concluded that the modified model could well predict the distributions and the average values of the liquid slug length and the Taylor bubble length along a narrow rectangular channel.

6. Conclusion

Using a high-speed video camera system, the evolution of gas–liquid two-phase slug flow in a vertical narrow rectangular channel is investigated and following conclusions can be drawn:

The velocity of the trailing Taylor bubble in the region undisturbed by the leading one could be reliably predicted by the Nicklin et al. (1962) correlation provided that C_0 is given by correlation of Ishii (1977) and the drift velocity is predicted by correlation of Sadatomi et al. (1982).

The Taylor bubble velocity is dependent on the liquid slug length ahead of it, and an empirical correlation is proposed based on the experimental data.

The length distributions of the Taylor bubbles and liquid slugs are positively skewed (log-normal distribution) at all measuring positions for all flow conditions. The mean lengths of the Taylor bubble and liquid slug gradually increase along the channel, and their distributions become more flat.

A model for predicting length distributions of the liquid slugs and Taylor bubbles along the channel, based on the model for circular tubes, is adapted for a vertical narrow rectangular channel. In general, the mean length and the overall shapes of the distributions are predicted well by the model.

Acknowledgements

The authors are profoundly grateful to the financial supports of the National Natural Science Foundation of China (Grant Nos.: 11175050, 51376052); the Fundamental Science on Nuclear Safety and Simulation Technology Laboratory, Harbin Engineering University; the Scientific Foundation of Returned Overseas Chinese Scholars, State Education Ministry as well as the Postdoctoral Foundation of Heilongjiang Province, China.

References

Aladjem Talvy, C., Shemer, L., Barnea, D., 2000. On the interaction between two consecutive elongated bubbles in a vertical pipe. Int. J. Multiphase Flow 26, 1905–1923.

Araújo, J.D.P., Miranda, J.M., Campos, J.B.L.M., 2013. Flow of two consecutive Taylor bubbles through a vertical column of stagnant liquid – a CFD study about the influence of the leading bubble on the hydrodynamics of the trailing one. Chem. Eng. Sci. 97, 16–33.

Bretherton, F.P., 1961. The motion of long bubbles in tubes. J. Fluid Mech. 10, 166–188.
Bendiksen, K.H., Zuber, N., 1984. An experimental investigation of the motion of long bubbles in inclined tubes. Int. J. Multiphase Flow 10, 467–483.
Bhusan, S., Ghosh, S., Das, G., Das, P.K., 2009. Rise of Taylor bubbles through narrow rectangular channels. Chem. Eng. J. 155, 326–332.
Barnea, D., Taitel, Y., 1993. A model for slug length distribution in gas–liquid slug flow. Int. J. Multiphase Flow 19, 829–838.
Bernicot, M., Drouffe, J.M., 1989. Slug length distribution in diphasic transport systems. In: Proceedings of the Fourth International Conference Multiphase flow. Nice, France, pp. 485–493.
Clanet, C., Heraud, P., Searby, G., 2004. On motion of bubbles in vertical tubes of arbitrary cross section: some complements to Dumitrescu-Taylor problem. J. Fluid Mech. 519, 359–376.
Cook, M., Behnia, M., 2000. Slug length prediction in near horizontal gas–liquid intermittent flow. Chem. Eng. Sci. 55, 2009–2018.
Campos, J.B.L.M., Guedes de Carvalho, J.R.F., 1988. An experimental study of the wake of gas slugs rising in liquids. J. Fluid Mech. 196, 27–37.
Dumitrescu, D.T., 1943. Stromung an einer Luftblase im senkrechten Rohr. Z. Angew. Math. Mech. 23, 139–149.
Davies, R.M., Taylor, G.I., 1950. The mechanics of large bubbles rising through extended liquids and through liquids in tubes. Proc. R. Soc. Lond. A 200, 375–390.
Dhulesia, H., Bernicot, M., Deheuvels, P., 1991. Statistical analysis and modelling of slug lengths. In: Proceedings of the Fifth International Conference on Multiphase Production, Cannes, France. BHRA, Cranfield, Beds, pp. 80–112.
Fabre, J., Liné, A., 1997. Slug flow. In: Hewitt, G.F., Shires, G.L., Polezhaef, Y.V. (Eds.), Encyclopedia of Heat Transfer. CRC Press, London, pp. 1015–1025.
Griffith, P., 1963. The prediction of low quality boiling void. ASME Preprint 63-HT-20.
Hibiki, T., Mishima, K., 2001. Flow regime transition criteria for upward two-phase flow in vertical narrow rectangular channels. Nucl. Eng. Des. 203, 117–131.
Ide, H., Kariyasaki, A., Fukano, T., 2007. Fundamental data on the gas–liquid two-phase flow in minichannels. Int. J. Therm. Sci. 46, 519–530.
Ishii, M., 1977. One-dimensional drift-flux model and constitutive equations for relative motion between phases in various two-phase flow regimes. ANL-77-47, USA.
Mishima, K., Hibiki, T., Nishihara, H., 1993. Some characteristics of gas–liquid flow in narrow rectangular ducts. Int. J. Multiphase Flow 19, 115–124.
Moissis, R., Griffith, P., 1962. Entrance effects in a two-phase slug flow. J. Heat Transfer 84, 29–39.
Maneri, C.C., Zuber, N., 1974. An experimental study of plane bubbles rising at inclination. Int. J. Multiphase Flow 1, 623–645.
Mayor, T.S., Pinto, A.M.F.R., Campos, J.B.L.M., 2007a. Hydrodynamics of gas–liquid slug flow along vertical pipes in the laminar regimes—experimental and simulation study. Ind. Eng. Chem. Res. 46, 3794–3809.
Mayor, T.S., Pinto, A.M.F.R., Campos, J.B.L.M., 2007b. Hydrodynamics of gas–liquid slug flow along vertical pipes in turbulent regime: a simulation study. Chem. Eng. Res. Des. 85, 1–17.
Mayor, T.S., Ferreira, V., Pinto, A.M.F.R., Campos, J.B.L.M., 2008a. Hydrodynamics of gas–liquid slug flow along vertical pipes in turbulent regime—an experimental study. Int. J. Heat Fluid Flow 29, 1039–1053.
Mayor, T.S., Pinto, A.M.F.R., Campos, J.B.L.M., 2008b. Vertical slug flow in laminar regime in the liquid and turbulent regime in the bubble wake—comparison with fully turbulent and fully laminar regimes. Chem. Eng. Sci. 63, 3614–3631.
Miller, I., Freund, J.E., 1965. Probability and Statistics for Engineers. Prentice-Hall, Englewood Cliffs, NJ.
McAdams, W.H., Woods, W.K., Heroman, L.C., 1942. Vaporization inside horizontal tubes-III, benzene–oil mixtures. Trans. ASME 64, 193.
Nicklin, D.J., Wilkes, J.O., Davidson, J.F., 1962. Two-phase flow in vertical tubes. Trans. Inst. Chem. Eng. 40, 61–68.
Nydal, O.J., Pintus, S., Andreussi, P., 1992. Statistical characterization of slug flow in horizontal pipes. Int. J. Multiphase Flow 18, 439–453.
Pinto, A.M.F.R., Coelho Pinheiro, M.N., Campos, J.B.L.M., 1998. Coalescence of two gas slugs rising in a co-current flowing liquid in vertical tubes. Chem. Eng. Sci. 53, 2973–2983.
Shemer, L., Barnea, D., 1987. Visualization of the instantaneous velocity profiles in gas–liquid slug flow. Phys. Chem. Hydrodyn. 8, 243–253.
Shemer, L., 2003. Hydrodynamic and statistical parameters of slug flow. Int. J. Heat Fluid Flow 24, 334–344.
Sadatomi, M., Sato, Y., Saruwatari, S., 1982. Two-phase flow in vertical noncircular channels. Int. J. Multiphase Flow 8, 641–655.
Sowinski, J., Dziubinski, M., Fidos, H., 2009. Velocity and gas-void fraction in two-phase liquid–gas flow in narrow mini-channels. Arch. Mech. 61, 29–40.
Satitchaicharoen, P., Wongwises, S., 2004. Two-phase flow pattern maps for vertical upward gas–liquid flow in mini-gap channels. Int. J. Multiphase Flow 30, 225–236.
Viana, F., Pardo, R., Yánez, R., Trallero, J.L., Joseph, D.D., 2003. Universal correlation for the rise velocity of long gas bubbles in round pipes. J. Fluid Mech. 494, 379–398.
van Hout, R., Barnea, D., Shemer, L., 2001. Evolution of statistical parameters of gas–liquid slug flow along vertical pipes. Int. J. Multiphase Flow 27, 1579–1602.
van Hout, R., Barnea, D., Shemer, L., 2002. Translational velocities of elongated bubbles in continuous slug flow. Int. J. Multiphase Flow 28, 1333–1350.
van Hout, R., Shemer, L., Barnea, D., 2003. Evolution of hydrody-namic and statistical parameters of gas–liquid slug flow along inclined pipes. Chem. Eng. Sci. 58, 115–133.
White, E.T., Beardmore, R.H., 1962. The velocity of rise of single cylindrical air bubbles through liquids contained in vertical tubes. Chem. Eng. Sci. 17, 351–361.
Wallis, G.B., 1969. One-Dimensional Two-Phase Flow. McGraw Hill, New York.
Wang, Y., Yan, C.Q., Sun, L.C., Xing, D.C., Yan, C.X., 2013a. Study on slug velocity of air-water two-phase flow in vertical narrow rectangular channel. At. Energy Sci. Technol. 47, 26–31 (in Chinese).
Wang, Y., Yan, C.Q., Sun, L.C., Yan, C.X., Xing, D.C., 2013b. Slug velocity in inclined narrow rectangular channel. CIESC J. 64, 4001–4007 (in Chinese).
Wang, Y., Yan, C.Q., Sun, L.C., Yan, C.X., 2014a. Characteristics of slug flow in a vertical narrow rectangular channel. Exp. Therm. Fluid Sci. 53, 1–16.
Wang, Y., Yan, C.Q., Sun, L.C., Yan, C.X., Tian, Q.W., 2014b. Characteristics of slug flow in a narrow rectangular channel under inclined conditions. Prog. Nucl. Energy 76, 26–35.
Wang, X., Guo, L.J., Zhang, X.M., 2006. Development of liquid slug length in gas–liquid slug flow along horizontal pipeline: experiment and simulation. Chin. J. Chem. Eng. 14, 626–633.
Wang, S.H., Zhang, H., Wang, J., 2009. Cryogenic liquid slug and Taylor bubble length distributions in an inclined tube. Chin. J. Chem. Eng. 17, 20–26.
Wang, C., Gao, P.Z., Tan, S.C., Xu, C., 2012. Effect of aspect ratio on the laminar-to-turbulent transition in rectangular channel. Ann. Nucl. Energy 46, 90–96.
Wilmarth, T., Ishii, M., 1997. Interfacial area concentration and void fraction of two-phase flow in narrow rectangular vertical channels. J. Fluids Eng. 19, 916–922.
Xia, G.D., Cui, Z.Z., Liu, Q., Zhou, F.D., Hu, M.S., 2009. A model for liquid slug length distribution in vertical gas–liquid slug flow. J. Hydrodyn. 21, 491–498.
Yan, C.X., Yan, C.Q., Sun, L.C., Wang, Y., Zhang, X.N., 2014. Slug behavior and pressure drop of adiabatic slug flow in a narrow rectangular duct under inclined conditions. Ann. Nucl. Energy 64, 21–31.
Zheng, D.H., Che, D.F., 2006. Experimental study on hydrodynamic characteristics of upward gas–liquid slug flow. Int. J. Multiphase Flow 32, 1191–1218.